JTTEE5 19:137–147
DOI: 10.1007/s11666-009-9422-2
1059-9630/$19.00 © ASM International

Corrosion Resistance of APS- and HVOF-Sprayed Coatings in the Al_2O_3-TiO_2 System

F.-L. Toma, C.C. Stahr, L.-M. Berger, S. Saaro, M. Herrmann, D. Deska, and G. Michael

(Submitted April 29, 2009; in revised form September 14, 2009)

In this article, the results of corrosion investigations performed on thermally sprayed ceramic coatings with different compositions in the Al_2O_3-TiO_2 system (Al_2O_3, Al_2O_3-3%TiO_2, Al_2O_3-40%TiO_2, and TiO_x) are presented. The coatings were deposited on corrosion-resistant steel substrates using atmospheric plasma spraying (APS) and high-velocity oxy-fuel (HVOF) spraying processes and characterized by means of optical microscopy, scanning electron microscopy (SEM), and x-ray diffraction (XRD). The corrosion properties were investigated in 1 N solutions of NaOH and H_2SO_4, at room temperature, 60 °C, and 85 °C, as well as in hydrothermal conditions with deionized water at 100 °C and 200 °C. The corrosion stability of the coatings depended on coating characteristics (spraying method, microstructure, and crystalline phase composition) and the corrosive environment (media, test temperature, and duration). In contrast to expectations, APS-sprayed coatings were found to be more corrosion-resistant than the HVOF-sprayed coatings. Addition of TiO_2 to Al_2O_3 increased the corrosion stability, especially for the HVOF-sprayed coatings. In this work, TiO_x coatings were found to be more corrosion-resistant than the Al_2O_3-based coatings.

Keywords Al_2O_3, Al_2O_3-3TiO_2, Al_2O_3-40TiO_2, TiO_x, corrosion resistance, corrosion test

1. Introduction

Thermal spray processes represent an important and rapidly growing group of surface modification technologies. Besides metals and hardmetals, ceramic materials are one of the most important for the preparation of thermally sprayed coating solutions. Atmospheric plasma spraying (APS) is traditionally the most common spray process for preparation of ceramic coatings due to their high melting temperatures. High-velocity oxy-fuel (HVOF) spraying, another widely used thermal spray process, is characterized by significantly lower process temperatures and higher particle velocities, resulting in coating formation from particles with higher kinetic energy. Coatings prepared by HVOF show lower porosity, higher bond strength, and lower roughness.

Al_2O_3 plays an important role both in the field of sintered materials and for thermally sprayed coatings. Al_2O_3 materials are widely used in industrial applications due to their good mechanical, wear, and anti-corrosion properties and high electrical resistance up to high temperatures. Whenever thermally sprayed Al_2O_3 coatings are used, regardless of the spray process used to prepare them, the typical properties of sintered Al_2O_3 ceramics are expected (Ref 1). A major difference between sintered Al_2O_3 and thermally sprayed Al_2O_3 coatings is that sprayed coatings are composed of different thermodynamically unstable forms of Al_2O_3 (e.g., γ- or δ-Al_2O_3), even though all commonly used feedstock powders are composed of α-Al_2O_3 (corundum), the only stable modification of Al_2O_3. This rather uncommon material behavior has been known for a long time and was described in detail by McPherson (Ref 2, 3). Thermally sprayed coatings are currently produced with these phase transformations being either ignored or accepted. Despite this transformation, coating properties are still acceptable for many applications. However, there are significant differences between these phases, e.g., in terms of long-term stability in humid environments. Several authors (Ref 4, 5) confirmed that the presence of the γ-phase combined with porosity and substrate characteristics drastically changes the corrosion properties of the coating compared with α-alumina. For sintered ceramics, it is also known that even a small level of impurities significantly modifies the corrosion process (Ref 6).

In many cases, there is a great need to obtain thermally sprayed coatings consisting of the α-phase. Various

This article is an invited paper selected from presentations at the 2009 International Thermal Spray Conference and has been expanded from the original presentation. It is simultaneously published in *Expanding Thermal Spray Performance to New Markets and Applications: Proceedings of the 2009 International Thermal Spray Conference*, Las Vegas, Nevada, USA, May 4-7, 2009, Basil R. Marple, Margaret M. Hyland, Yuk-Chiu Lau, Chang-Jiu Li, Rogerio S. Lima, and Ghislain Montavon, Ed., ASM International, Materials Park, OH, 2009.

F.-L. Toma, C.C. Stahr, L.-M. Berger, and **S. Saaro**, Fraunhofer Institute for Material and Beam Technology (Fh-IWS), Winterbergstrasse 28, D-01277 Dresden, Germany; **C.C. Stahr**, W.C. Heraeus GmbH, Thin Film Materials Division, Wilhelm-Rohn-Strasse 25, 63450 Hanau, Germany; and **M. Herrmann, D. Deska,** and **G. Michael**, Fraunhofer Institute for Ceramic Technologies and Systems (Fh-IKTS), Winterbergstrasse 28, D-01277 Dresden, Germany. Contact e-mail: filofteia-laura.toma@iws.fraunhofer.de.

methods of post-spray treatment, e.g., annealing, laser remelting, or sealing, were proposed for improvement of the properties of thermally sprayed alumina coatings in different corrosive environments (Ref 7-10).

Titanium oxide is another ceramic material extensively studied and used due to its multifunctional character. For example, titanium oxide is applied or under investigation for use in coatings designated for electrical, solid lubrication, mechanical, biomedical, or photocatalytic applications (Ref 11, 12). The use of titanium oxide in different applications is closely connected with the existence of different titanium dioxide modifications and the formation of suboxides. Hayfield (Ref 13) confirmed that titanium oxide ceramics show a high corrosion resistance, which increases with increasing O/Ti ratio. The oxygen deficiency degree of the thermally sprayed coatings is linked to the properties of the feedstock spray powder and the spray process.

Additions of TiO_2 in the range of 3-40 wt.% to alumina powder are frequently used in thermal spraying (Ref 14, 15). Through the formation of a eutectic composition, the TiO_2 addition to Al_2O_3 involves the formation of a liquid phase at a significantly lower temperature, with the amount depending on the TiO_2 content. At a content of 44 mass% TiO_2, the compound Al_2TiO_5 (aluminum titanate, mineralogical name: tialite) is formed; this presents interesting properties that differ from those of both Al_2O_3 and TiO_2. It was confirmed that the addition of TiO_2 to alumina (Ref 5, 16, 17) or use of Al_2TiO_5 (Ref 18) prevents corrosion in dilute acids.

The spray powders are available both as mechanical mixtures of Al_2O_3 and TiO_2 powders and as jointly (prealloyed) fused and crushed feedstock powders. For these reasons, the phase composition of the coating consists of a mixture of different phases of Al_2O_3, TiO_2, and Al_2TiO_5 (Ref 19). In the evaluation of the coating properties, this fact is often neglected and the coatings are only designated as Al_2O_3-TiO_2 coatings.

The work presented in this article was performed as part of a larger project on corrosion resistance of oxide coatings. An overview of the project results has been given by Berger et al. (Ref 20); preliminary results have been published elsewhere (Ref 21). Normally, when the corrosion resistance of thermally sprayed coatings is discussed, it refers to the ability of the coatings to protect the substrates from corrosion. The results presented in this article give details on the corrosion properties of APS- and HVOF-sprayed coatings prepared from feedstock spray powders with different compositions in the Al_2O_3-TiO_2 system (Al_2O_3, Al_2O_3-3wt.%TiO_2, Al_2O_3-40wt.%TiO_2, and TiO_x) in basic, acidic, and hydrothermal conditions at different temperatures. The corrosion resistance of the Al_2TiO_5 coatings investigated in this study (Refs 20, 21) was detrimentally affected by the high content of SiO_2 and other elements present in the feedstock powder. For this reason, these results are not included in this article.

Knowledge of the behavior in the spray process and investigation of the corrosion resistance of the coatings enable targeted knowledge-based materials and process selection for thermally sprayed coatings for protection of metallic substrates in different corrosive media.

2. Experimental

2.1 Feedstock Powders and Coating Preparation

Commercial fused and crushed powders Al_2O_3 (99.7 wt.% purity), Al_2O_3-3%TiO_2, Al_2O_3-40%TiO_2, and TiO_x (Ceram GmbH, Albbruck-Birndorf, Germany) with appropriate particle size distributions for both APS ($-40+10$ μm) and HVOF spraying ($-25+5$ μm) were used for coating preparation. When in chemical equilibrium, the composition Al_2O_3-40%TiO_2 is characterized by the presence of Al_2O_3 and Al_2TiO_5. For the TiO_x powder, a mass gain of 5.7% was determined by thermogravimetric analysis in streaming air, the values of x being estimated to be 1.73 for this powder (Ref 22). The phase compositions of these powders and the corresponding coatings were characterized by x-ray diffraction and are discussed below.

APS coatings were sprayed with a F6 plasma gun (GTV mbH, Luckenbach, Germany) using an Ar/H_2 plasma gas mixture. HVOF coatings were sprayed with a Top Gun system (GTV mbH) using ethylene as a fuel gas. The spray parameters were optimized in order for coatings with low porosity to be obtained. The main spray parameters are compiled in Table 1.

Coatings were deposited on round substrates 25 mm in diameter. Corrosion-resistant substrates were selected in this study so that just the behavior of the coatings in different corrosive media could be studied. The initially used steel 1.4031 (X40Cr13) proved to be adequately stable only in basic media. For this reason, stainless steel 1.4462 (X2CrNiMoN 22-5-3) was used as a substrate in most of the tests. All of the substrates were thoroughly cleaned, degreased, and grit-blasted with corundum prior to coating. The coating thickness was about 200-250 μm. All specimens were used in the as-sprayed condition, without any further machining or sealing, for the corrosion tests.

2.2 Corrosion Tests

The corrosion stability of thermally sprayed coatings was investigated in different corrosive media: 1 N aqueous solution of NaOH and H_2SO_4, respectively, as well as deionized water. The corrosion tests were carried out in a 1.5-L Teflon reaction vessel equipped with Teflon sample holders (Ref 20, 23). For the investigation of the corrosion

Table 1 Main spray parameters

APS		HVOF	
Ar/H_2 (splm*)	40/13	C_2H_4/O_2 (slpm)	90/270; 90/295
Plasma power (kW)	55-62		
Powder feed rate (g min^{-1})	30-33	Powder feed rate (g min^{-1})	25-30
Ar carrier gas (slpm)	4	Ar, carrier gas (slpm)	28
Spray distance (mm)	115	Spray distance (mm)	150

* Standard liter per minute

behavior of the sprayed coatings, a special sample holder was implemented (Ref 20). This kind of holder only allowed a defined sample surface to come into contact with the corrosion medium. Testing with deionized water was realized in an autoclave also equipped with a Teflon reaction vessel.

The corrosion tests in NaOH and H_2SO_4 were performed at room temperature (23 °C), 60 °C, and 85 °C. The basic and acidic solutions were continuously stirred and completely changed after certain times to avoid strong enrichment of dissolved components. The hydrothermal corrosion tests with deionized water were carried out at 150 °C and 200 °C. Before and after the corrosion experiments the samples were cleaned with acetone for 10 min, rinsed with deionized water, dried at 150 °C for 2 h, and weighed with a microbalance (0.01-mg accuracy) after a 2-h cooling period. The change in coating mass was measured at intervals up to 300 h in the corrosive media. For each coating series, the average mass loss was obtained using the results of corrosion tests performed on 2 to 5 samples. The matrix of corrosion investigations on the thermally sprayed coatings is given in Table 2.

2.3 Microstructural and Phase Characterization

Coating microstructure was investigated before and after the corrosion experiments by optical microscopy, SEM (JEOL JSM-6300 microscope and Leica Stereoscan 290), and EDX analysis on metallographically polished cross sections and surfaces. The crystalline phase compositions of the powders and the coatings were analyzed by x-ray diffraction using an XRD 7 (GE Inspection Technologies) diffractometer. Measurements were carried out in the θ-2θ step scan mode using CuKα radiation and a step size of 0.05.

Table 2 Matrix of corrosion investigations

Corrosion media	Al_2O_3		Al_2O_3-3TiO_2		Al_2O_3-40TiO_2		TiO_x	
	APS	HVOF	APS	HVOF	APS	HVOF	APS	HVOF
1 N H_2SO_4								
RT	x	x			x			
60 °C	x	x			x	x		
85 °C	x	x	x	x	x	x	x	x
1 N NaOH								
RT	x	x			x			
85 °C	x	x	x	x	x	x	x	x
Deionized H_2O								
150 °C	x	x			x	x		
200 °C	x	x			x	x	x	x

3. Results and Discussion

3.1 Phase Compositions of Powders and Coatings

Typical XRD patterns of the feedstock powders are presented in Fig. 1. The spray powders of composition Al_2O_3 and Al_2O_3-3TiO_2 consisted nearly solely of corundum (α-Al_2O_3, JCPDS card no. 46-1212). Traces of β-Al_2O_3 (JCPDS card no. 10-0414) could be detected in the Al_2O_3 feedstock powder. In the HVOF fraction of the Al_2O_3-3TiO_2 powder, small traces of rutile (JCPDS card no. 21-1276) were found. In the Al_2O_3-40TiO_2 powder, the Al_2TiO_5 phase with lattice parameters shifted in relation to those of the Al_2TiO_5 standard (JCPDS card no. 41-0258) were found to exist. This shift was due to the formation and dissolution of Ti_3O_5 in Al_2TiO_5 in reducing conditions. The phase that arose can be described by the formula $Al_{2-x}Ti_{1+x}O_5$. Stoichiometric TiO_2 was detected in the form of rutile and various suboxides in the TiO_x powder.

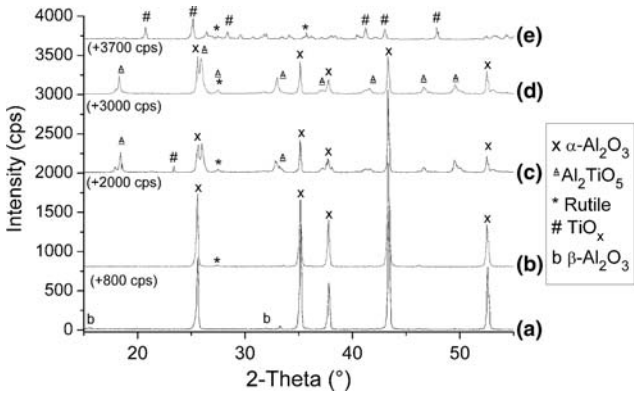

Fig. 1 XRD patterns of feedstock spray powders: (a) Al_2O_3 for HVOF; (b) Al_2O_3-3TiO_2 for HVOF; (c) Al_2O_3-40TiO_2 for APS; (d) Al_2O_3-40TiO_2 for HVOF; and (e) TiO_x for HVOF

Table 3 Phase compositions of feedstock powders and thermally sprayed coatings

Material	Phase composition of powder suitable for		Phase composition of sprayed coating	
	APS	HVOF	APS	HVOF
Al_2O_3	α-Al_2O_3, β-Al_2O_3[#]		γ-Al_2O_3, α-Al_2O_3	γ-Al_2O_3, α-Al_2O_3, β-Al_2O_3[#]
Al_2O_3-3TiO_2	α-Al_2O_3	α-Al_2O_3, rutile[#]	γ-Al_2O_3, α-Al_2O_3	γ-Al_2O_3, α-Al_2O_3
Al_2O_3-40TiO_2	α-Al_2O_3, Al_2TiO_5*, rutile[#], TiO_{2-x}[#]	α-Al_2O_3, Al_2TiO_5*, rutile[#]	Al_2TiO_5*, γ-Al_2O_3, α-Al_2O_3, TiO_{2-x}	γ-Al_2O_3, TiO_{2-x}, Al_2TiO_5*, Ti_6O_{11},α-Al_2O_3, Ti_9O_{17}
TiO_x	Ti_4O_7, Ti_3O_5, rutile, other suboxides	Ti_3O_5, Ti_4O_7, rutile, Ti_5O_9, other suboxides	Titanium suboxides, rutile, anatase	Rutile*, anatase[#]

"*" indicates shifted lattice parameters with respect to the standard, "[#]" indicates traces

An overview of the crystalline phases of feedstock powders and sprayed coatings is given in Table 3. Changes in the phase composition were observed in the coatings compared with the feedstock powders (Fig. 2). In the case of sprayed coatings, both α-Al_2O_3 and γ-Al_2O_3 (JCPDS card no. 10-0425) were detected. Up to a TiO_2 content of 3% by mass, the coatings consisted nearly exclusively of α-Al_2O_3 and γ-Al_2O_3, with γ-Al_2O_3 being the main phase. Traces of β-Al_2O_3 were found in the HVOF coating. For the coatings sprayed from the Al_2O_3-40TiO_2 feedstock powder, TiO_2 was found both in the HVOF and in the APS coating in the form of rutile. Additional peaks indicated that the integral oxygen loss was greater in the APS coating than in the HVOF coating. The Al_2TiO_5 peaks in the Al_2O_3-40TiO_2 coatings were shifted with respect to the standard peaks. As in the case of the powders, this can be explained by the formation of an $Al_{2-x}Ti_{1+x}O_5$ solid solution consisting of Al_2TiO_5 and Ti_3O_5. The lattice parameters were shifted more than they were in the feedstock powders due to additional oxygen loss occurring during the spray process. The shift of the APS peaks was greater than those of the HVOF-sprayed coatings. The APS- and HVOF-sprayed TiO_x coatings showed different phase compositions. Whereas rutile appeared as the main crystalline phase and anatase (JCPDS card no. 21-1272) as

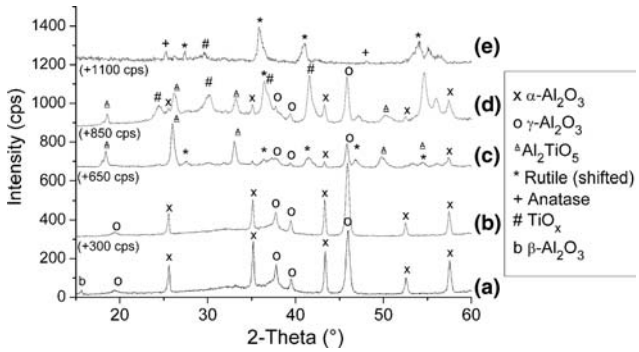

Fig. 2 XRD patterns of sprayed coatings: (a) Al_2O_3 HVOF; (b) Al_2O_3-3TiO_2 HVOF; (c) Al_2O_3-40TiO_2 APS; (d) Al_2O_3-40TiO_2 HVOF; and (e) TiO_x APS

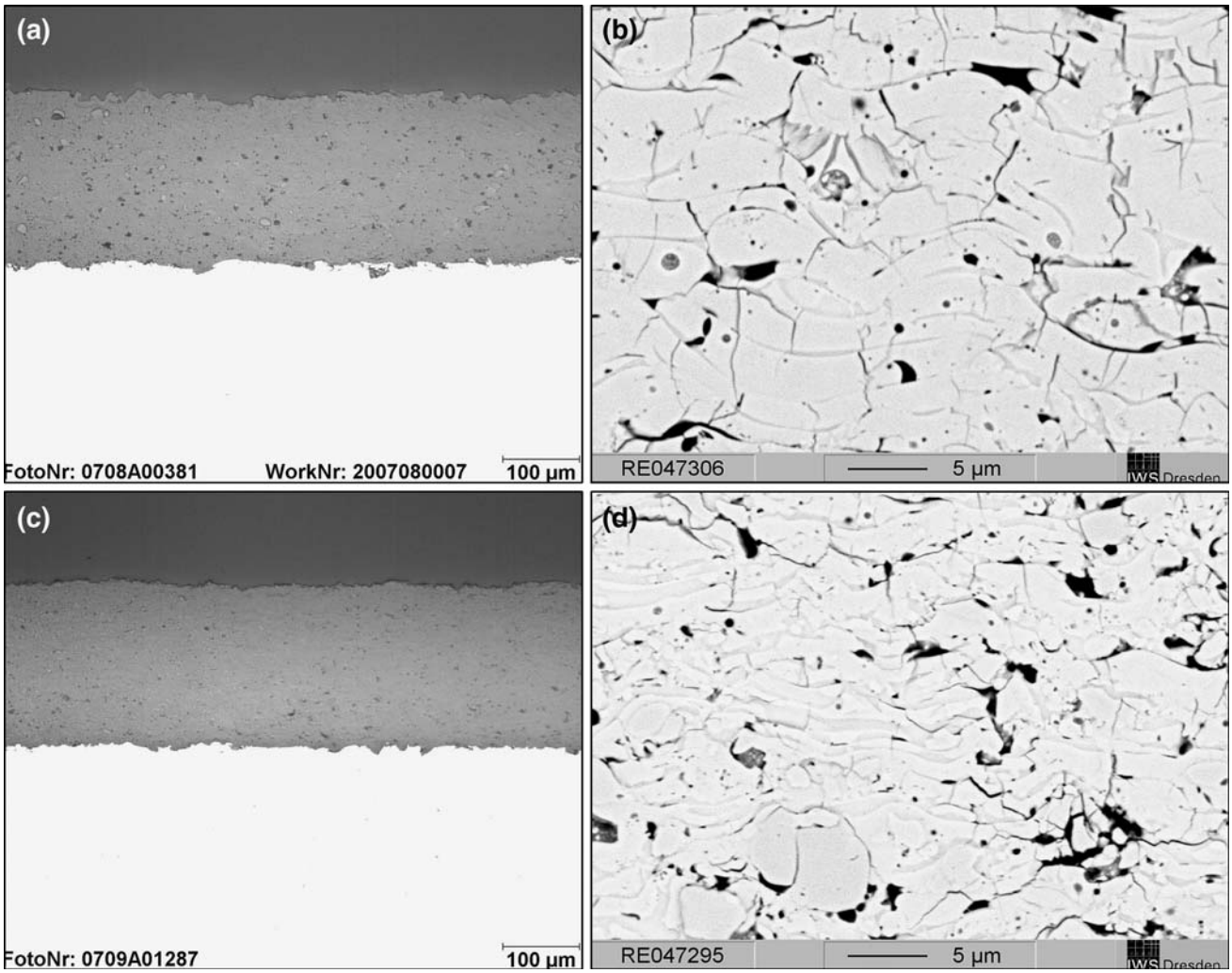

Fig. 3 Optical micrographs and SEM micrographs of sprayed Al_2O_3 coatings: (a, b) APS and (c, d) HVOF

a minor phase in the HVOF-sprayed coatings, titanium suboxides were the main phases and rutile and anatase minor phases due to reduction by hydrogen as a plasma gas component in the APS coatings.

The corundum (α-Al_2O_3) content in the coatings was found to depend on the TiO_2 content in the spray powders and the spray process. With increasing TiO_2 content in the feedstock powder, the corundum content decreased in HVOF coatings from about 42% (as determined in the Al_2O_3 coatings) to 26% (in the Al_2O_3-40TiO_2 coatings). Contrary to this, the α-Al_2O_3 ratio increased slightly in the APS coatings with increasing TiO_2 content: from 10% in the Al_2O_3 coatings to 17% in the Al_2O_3-40TiO_2 coatings.

3.2 Coating Microstructures

Both APS- and HVOF-sprayed Al_2O_3 coatings appeared to be dense and homogeneous in the optical micrographs shown in Fig. 3(a) and (c). However, SEM micrographs taken at high magnifications and contrast levels (Fig. 3b, d) showed that these apparently dense coatings actually contained fine networks of pores, microcracks, and unmelted particles. These microcracks and pores can affect the corrosion properties of coatings in such a way that the corrosive media can reach the substrate and degrades it.

Al_2O_3-3TiO_2-sprayed coatings also appeared to be homogeneous and dense in the optical micrographs (Fig. 4a), whereas the Al_2O_3-40TiO_2 presented the typical multiphase microstructure (Fig. 4b). In the optical micrographs, APS-sprayed TiO_x coatings showed different gray scales due to the different Ti/O ratios throughout the coatings (Fig. 4c). Use of an Ar/H_2 plasma gas mixture in the APS process resulted in both oxygen loss by reduction with hydrogen and oxygen uptake by oxidation due to atmospheric conditions, with the O/Ti-ratio differing locally in the coating. This phenomenon was less pronounced in the HVOF-sprayed TiO_x coatings (Fig. 4d).

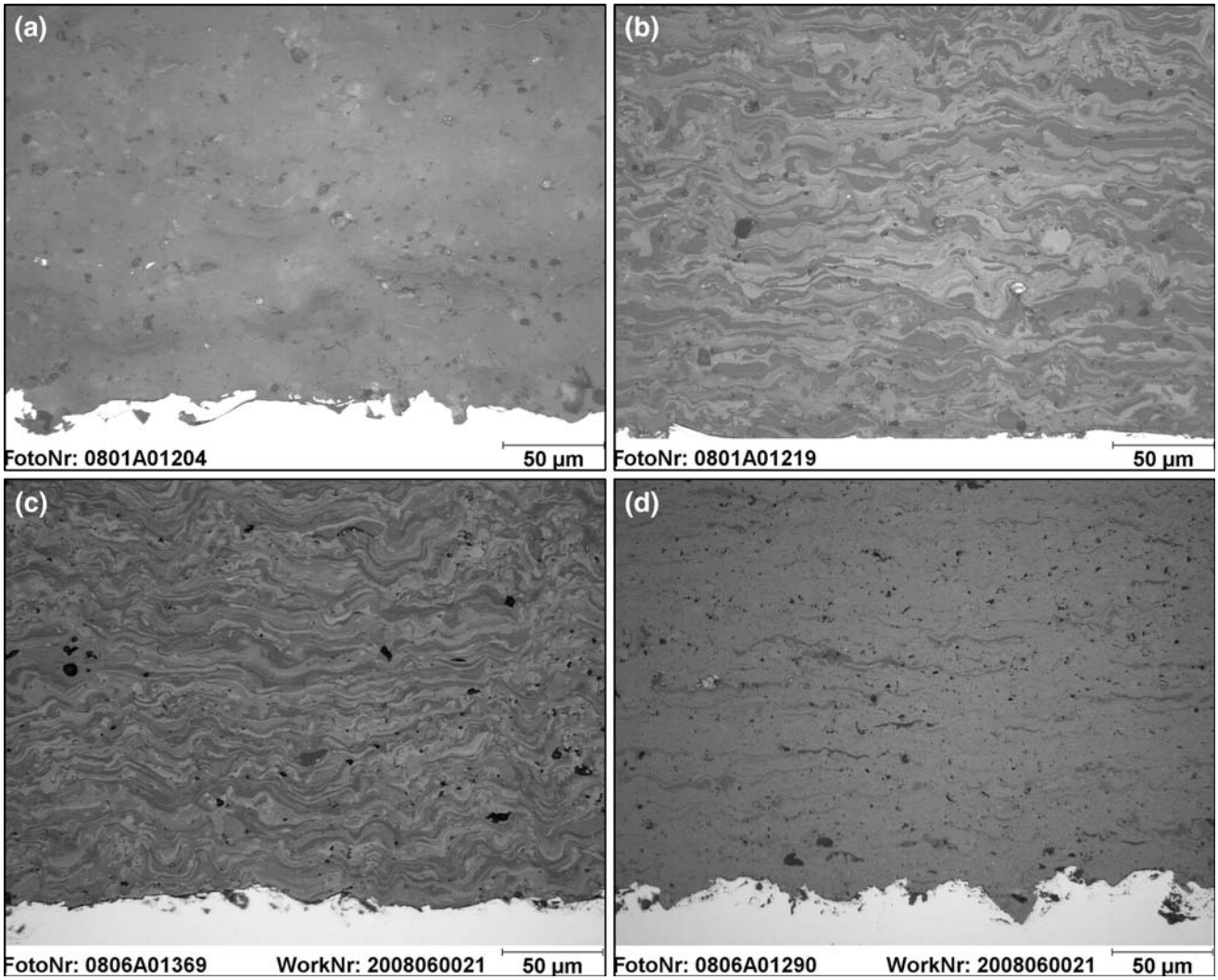

Fig. 4 Optical micrographs of: (a) APS-sprayed Al_2O_3-3TiO_2 coating; (b) APS-sprayed Al_2O_3-40TiO_2 coating; (c) APS-sprayed TiO_x coating; and (d) HVOF-sprayed TiO_x coating

From the measurements of the electrical resistivity of the coatings in an electrolyte, it was concluded that the porosity, which reaches the substrate (i.e., connected porosity) was in the range of 1 to 6% (Ref 20). To avoid the influence of the substrate corrosion, corrosion-resistant steels were selected in this study, so that just the behavior of the coatings in different corrosive media could be studied.

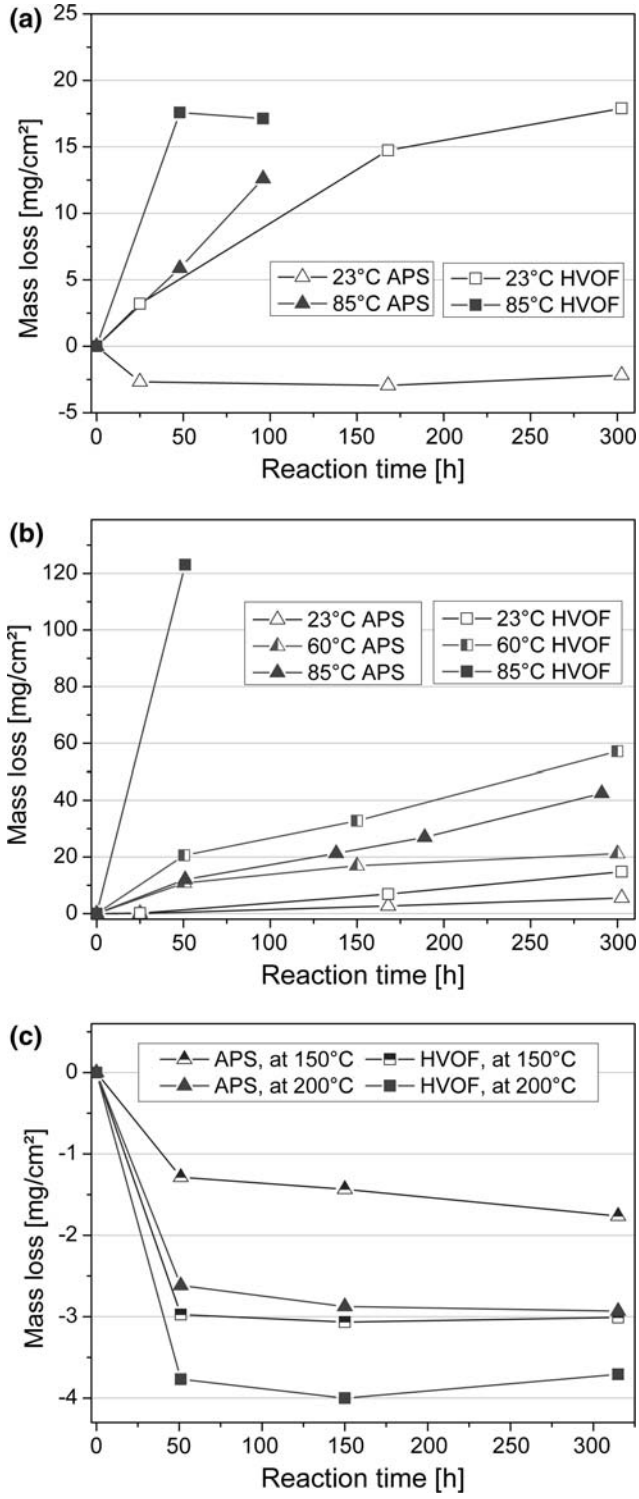

Fig. 5 Mass losses of Al_2O_3 coatings during testing at various temperatures in: (a) 1 N NaOH; (b) 1 N H_2SO_4; and (c) deionized water at different temperatures

3.3 Corrosion Resistance of Thermally Sprayed Coatings

3.3.1 Al_2O_3 Coatings. The corrosion resistance of the Al_2O_3 coatings depended on the spray process and the corrosion media (Fig. 5). Comparison of the APS- and HVOF-Al_2O_3 coatings that underwent corrosion tests in basic media (shown in Fig. 5a) reveals the fundamentally different behaviors of the two groups of coatings. Whereas the APS-sprayed coatings exhibited a slight mass gain at room temperature (which can be attributed to the formation of hydroxides), the HVOF-sprayed coatings

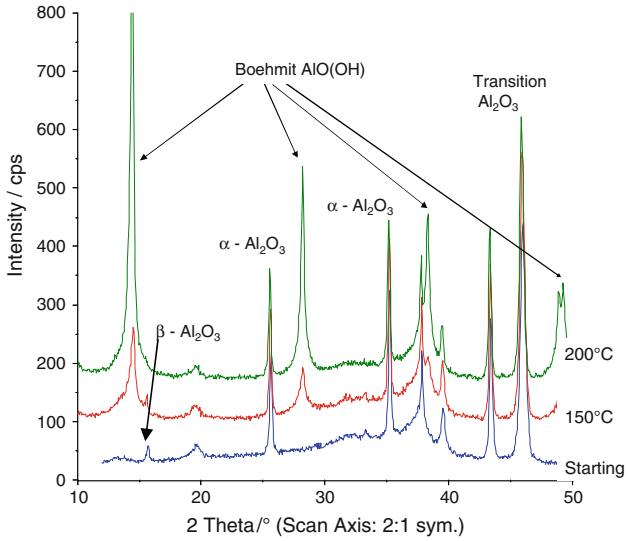

Fig. 6 Formation of the boehmite phase in the Al_2O_3-sprayed coatings during hydrothermal corrosion at 150 °C and 200 °C

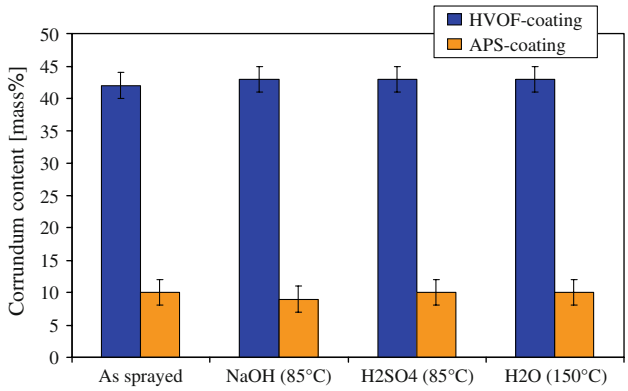

Fig. 7 Corundum contents (with respect to total crystalline fraction of Al_2O_3) in the as-sprayed coatings and in the coatings after 300-h testing in different corrosive media

showed a significant mass loss resulting from corrosion. Holding of the Al_2O_3 coatings in NaOH at 85 °C led to a high mass loss. The APS coatings exhibited a lower mass loss due to corrosion than the HVOF coatings did, even in acidic media (Fig. 5b). This trend became more pronounced as the temperature increased. At 85 °C, the test had to be discontinued for HVOF-sprayed coatings after 50 h due to the extremely high mass loss that occurred. The sprayed Al_2O_3 coatings exhibited good hydrothermal stability at temperatures up to 200 °C (Fig. 5c). The coatings even showed a slight mass gain. This gain can be attributed to the formation of hydroxides (i.e., boehmite: AlO(OH)), as was the case for testing in basic media. The formation of the boehmite phase during hydrothermal corrosion was also observed in the XRD patterns of the tested coatings, as can be seen in Fig. 6. These hydroxides presumably form a protective barrier preventing further corrosion. The boehmite can only be dissolved in a strong base at elevated temperatures.

Several authors (Ref 4, 24) concluded from their investigations that γ-Al_2O_3 is less stable in corrosive media than α-Al_2O_3 is. Baumgarten et al. (Ref 25) showed that γ-Al_2O_3 strongly dissolves in acidic media with a pH of less than 4 as well as in basic media with a pH of greater than 10; in neutral solutions (pH = 7), the solubility (dissolution) of γ-Al_2O is the lowest. Similar results have been found by Harju et al. (Ref 24) for plasma-sprayed alumina coatings.

With the exception of the hydrothermal conditions, all conditions yielded a lower corrosion resistance for the HVOF coatings than for the APS coatings, in spite of the fact that the α-content was higher in the HVOF coatings than in the APS coatings. The XRD investigations of the Al_2O_3 coatings after testing in NaOH, H_2SO_4, and deionized water showed that the ratio of the α-phase to the γ-phase remained constant (Fig. 7). This might indicate that corundum particles were depleted from the coating after the surrounding transition aluminas were dissolved. The finer microstructures of the HVOF coatings could also play a role in this.

The microstructural investigations showed corroded coatings with spongy microstructures after 300-h testing in H_2SO_4 (Fig. 8). However, this specific structure was not observed after testing in NaOH or in deionized water.

3.3.2 TiO_x Coatings. Figure 9 summarizes the corrosion behavior of the TiO_x coatings in NaOH, H_2SO_4, and hydrothermal conditions. Compared with the Al_2O_3 coatings, the TiO_x showed a higher corrosion resistance in acidic media. The good stability of plasma-sprayed titanium oxide coatings has also been mentioned by Harju et al. (Ref 24). One difference between TiO_x APS- and HVOF-sprayed coatings was seen after testing in H_2SO_4 at 85 °C. The APS-sprayed coatings exhibited a low mass loss in these conditions, whereas the HVOF-sprayed coatings showed a mass gain. The differences between the APS and HVOF coatings were caused by the differences in their phase compositions. Rutile was the main phase in the HVOF coatings, whereas titanium suboxides were the major components of the APS coatings. During the corrosion process no other phases were formed. Hence, it can be concluded from the investigations that the titanium suboxides have a slightly lower stability in acids than rutile does. During 300-h testing in hydrothermal conditions at 200 °C no mass changes for the TiO_x coatings were recorded.

3.3.3 Al_2O_3-TiO_2 Coatings. For the two compositions in the Al_2O_3-TiO_2 system, the trend in which the HVOF coatings exhibited a higher mass loss than the APS-sprayed coatings did also existed (Fig. 10). After testing for 300 h in a 1 N NaOH solution at 85 °C, the APS Al_2O_3-40TiO_2 coatings exhibited a slight mass gain compared with the APS-sprayed Al_2O_3 coating (Fig. 10a).

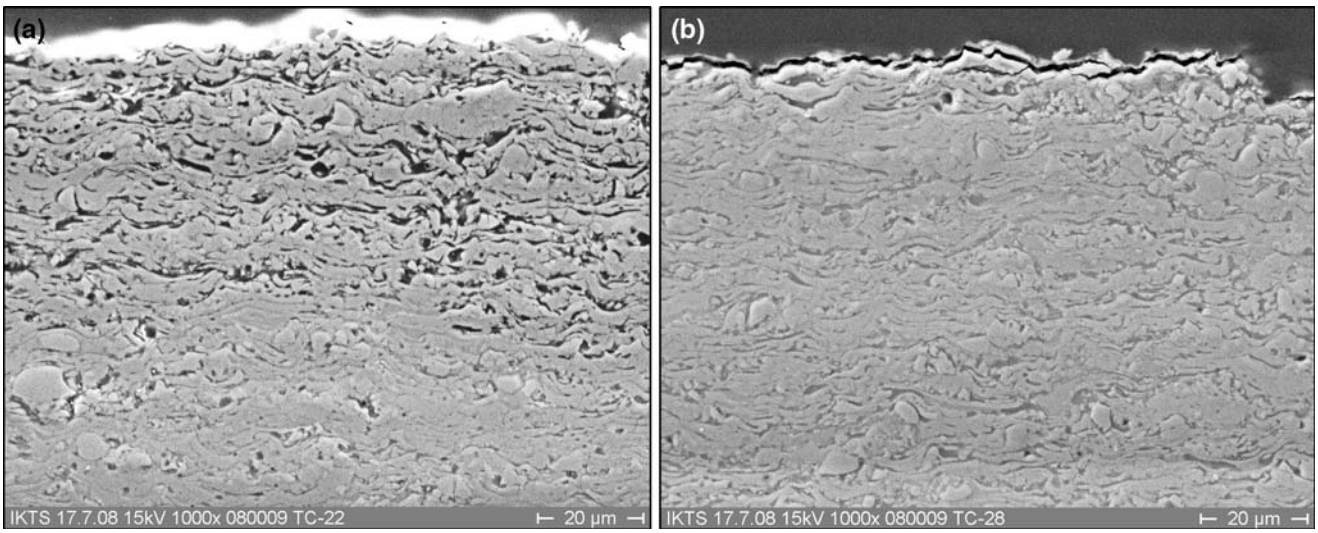

Fig. 8 SEM micrographs of corroded HVOF-sprayed Al_2O_3 coatings after 300-h testing in: (a) H_2SO_4 at 60 °C and (b) deionized water at 150 °C

The basic corrosion resistance increased with increasing TiO_2 content. In the HVOF-sprayed Al_2O_3-40TiO_2 coatings, after an initial mass loss, the corrosive attack decreased significantly and stabilization was achieved.

In an acidic medium at 85 °C, the corrosive attack decreased with increasing nominal TiO_2 content in the starting powder (Fig. 10b). The Al_2O_3-3TiO_2 coatings represented an exception to this rule. In acidic media, the corrosion resistance of the Al_2O_3-40TiO_2 coatings depended to a lesser extent on the spray process.

In the hydrothermal testing conditions, the Al_2O_3-40TiO_2 coatings showed good corrosion resistance (mass gain during the test due to boehmite formation), although this corrosion resistance was slightly lower than that of unalloyed Al_2O_3 coatings (Fig. 10c).

Compared with pure Al_2O_3 coatings, HVOF-sprayed coatings with additions of TiO_2 to the feedstock powders exhibited improved corrosion stability. Studies performed on bulk ceramics have shown that the corrosion stability of the Al_2O_3 ceramics decreases with increasing TiO_2 content (Ref 20). In the case of sprayed coatings, additions of TiO_2 increase the processability of alumina through the formation of a eutectic melt and consequently allow the formation of a liquid phase at the eutectic temperature, which is of particular importance during HVOF spraying. In the HVOF coatings, the content of the α-Al_2O_3 phase decreased with increasing TiO_2 content, but the coatings showed a denser microstructure. In the case of APS coatings, where the α-Al_2O_3 phase content increased with increasing TiO_2 content, the corrosion stability was practically unchanged. Thus, it can be concluded that the coating microstructure plays a more important role in corrosion resistance than the phase composition does.

As in the case of unalloyed Al_2O_3 coatings, XRD investigations of the corroded Al_2O_3-TiO_2 coatings showed that the ratio of the α-phase to the γ-phase remained constant; however, the Al_2TiO_5 phase was no longer detected after acidic corrosion at 85 °C.

After corrosion tests the coating microstructures were investigated. SEM micrographs and EDX analysis indicated that the aluminum-containing phases in the Al_2O_3-TiO_2 coatings were selectively attacked during acidic corrosion. An example for the HVOF Al_2O_3-40TiO_2 coatings after 300 h in H_2SO_4 solution at 85 °C is given in Fig. 11. The corroded coating presented a spongy microstructure in which the selective corrosive attack was

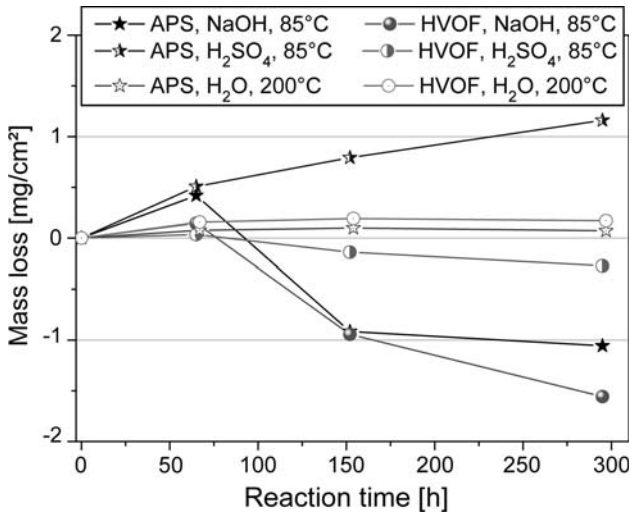

Fig. 9 Behavior of titanium oxide coatings during corrosion testing in NaOH and H_2SO_4 at 85 °C and hydrothermal conditions at 200 °C

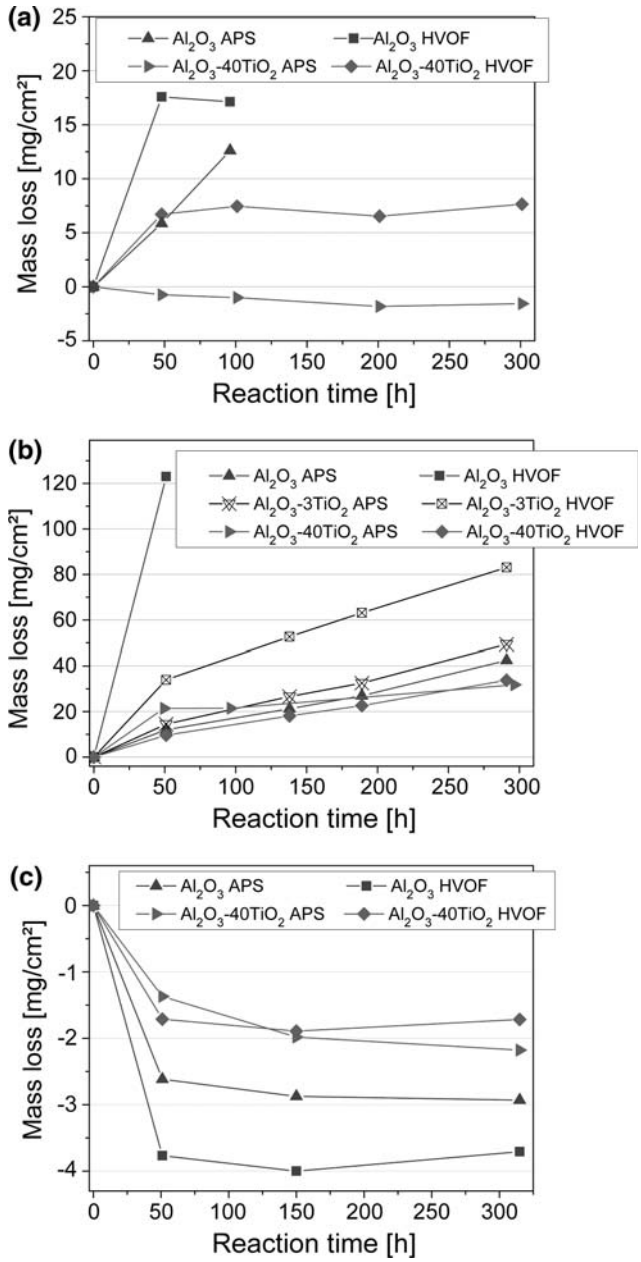

Fig. 10 Mass losses of binary Al_2O_3-TiO_2 coatings during testing in: (a) 1 N NaOH at 85 °C; (b) 1 N H_2SO_4 at 85 °C; and (c) deionized water at 200 °C

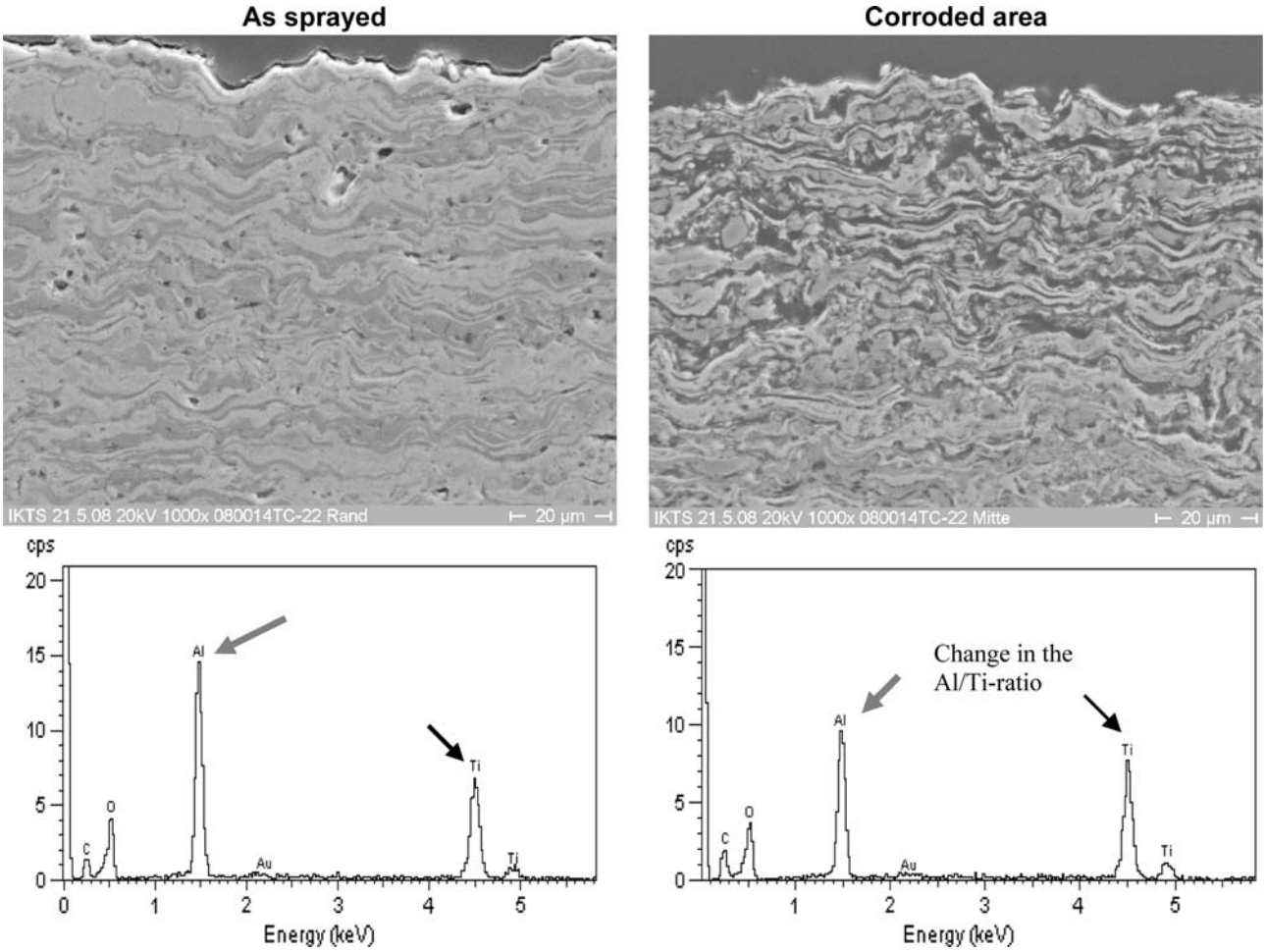

Fig. 11 Cross-sectional micrographs and EDX analysis of the HVOF Al_2O_3-40TiO_2 coating before (left) and after (right) 300-h corrosion test in 1 N H_2SO_4 solution at 85 °C

clearly visible. EDX analysis showed that the Al/Ti ratio was changed by dissolution of Al during exposure to the H_2SO_4 solution. Harju et al. (Ref 24) also found a higher chemical stability for TiO_2 (even though it is oxygen-deficient) than for alumina. Furthermore, it was stated by these authors that the coatings sprayed from mechanically mixed Al_2O_3-13TiO_2 powders contained Al_2O_3 particles covered by TiO_2 layers, which prevented the Al_2O_3 phase from dissolving.

The XRD analysis of the corroded coatings performed in this study showed the complete dissolution of the nonstoichiometric Al_2TiO_5 phase during corrosion. As already mentioned, the influence of the TiO_2 content in the APS-sprayed coatings on the corrosion resistance was relative low. In conclusion, the main factor in the enhancement of the corrosion resistance was the modified coating microstructure, rather than the chemical stability of the titanium oxide.

Investigations of corroded surfaces confirmed that the coatings exhibited different corrosion behavior in different corrosive environments. Figure 12 shows images of the surfaces of APS and HVOF Al_2O_3-40TiO_2 coatings. At a high magnification, the corrosive attack was very noticeable for the surfaces held in acidic media (presence of cavities on surface similar to those observed in pitting corrosion), in contrast to the coatings held in NaOH.

4. Summary and Conclusions

In the present work, the corrosion properties of APS- and HVOF-sprayed ceramic coatings prepared from feedstock powders with different compositions in the Al_2O_3-TiO_2 system (Al_2O_3, Al_2O_3-3wt.%TiO_2, Al_2O_3-40wt.%TiO_2, and TiO_x) in basic, acidic, and hydrothermal conditions at different temperatures was systematically investigated. The corrosion resistance of Al_2O_3 coatings prepared using HVOF spraying was lower than that of the APS coatings. Addition of TiO_2 to Al_2O_3 increased the stability of the thermally sprayed coatings, especially for the HVOF-sprayed coatings. The results showed the significant influence of the microstructure and the phase composition on the corrosion resistance of the coatings.

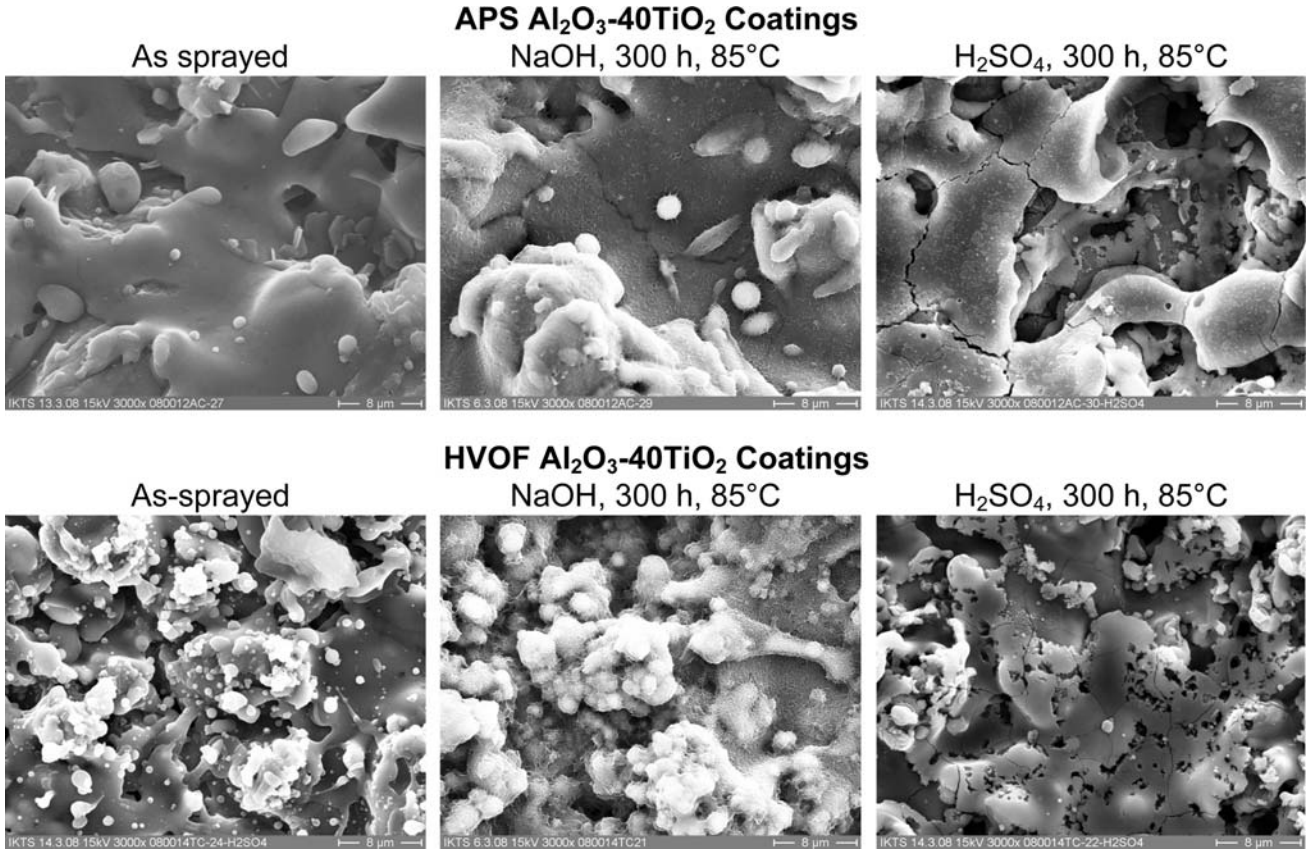

Fig. 12 SEM surface images of corrosive attack of APS and HVOF Al_2O_3-40TiO_2 coatings at different magnifications after 300-h testing at 85 °C in NaOH and in H_2SO_4

Of the coatings and conditions investigated in this work, the TiO_x sprayed coatings exhibited the best stability in the corrosive media.

Although not all relationships between coating structure and corrosion resistance could be clarified in this work, the results form a good basis for coating selection in different corrosion environments.

Acknowledgments

This work was part of the DVS research project ''Corrosion of thermally sprayed oxide-ceramic coatings'' (AiF No. 14.966 B), funded via AiF by the Federal Ministry of Economics and Technology within the framework of the program for promotion of ''Industrial Joint Research (IGF).'' The authors gratefully acknowledge this funding. Thanks are also due to Ms. B. Wolf (Fh-IWS) for metallographic sample preparation.

References

1. L.-M. Berger, C.C. Stahr, F.-L. Toma, G.C. Stehr, and E. Beyer, Ausgewählte Entwicklungstendenzen bei der Herstellung thermisch gespritzter keramischer Schichten (Selected Trends in the Preparation of Thermally Sprayed Ceramic Coatings), *Jahrbuch Oberflächentechnik 2007*, Bd. 63, R. Suchentrunk, Ed., Eugen G. Leuze Verlag, 2007, p 71-84 (in German)
2. R. McPherson, Formation of Metastable Phases in Flame- and Plasma-Prepared Alumina, *J. Mater. Sci.*, 1973, **8**(6), p 851-858
3. R. McPherson, On the Formation of Thermally Sprayed Alumina Coatings, *J. Mater. Sci.*, 1980, **15**(12), p 3141-3149
4. D. Yan, J. He, J. Wu, W. Qiu, and J. Ma, The Corrosion Behaviour of a Plasma Spraying Al_2O_3 Ceramic Coating in Dilute HCl Solution, *Surf. Coat. Technol.*, 1997, **89**(1-2), p 191-195
5. E. Çelik, A.S. Demirkiran, and E. Avci, Effect of Grit Blasting on the Corrosion Behaviour of Plasma-Sprayed Al_2O_3 Coatings, *Surf. Coat. Technol.*, 1999, **116-119**, p 1061-1064
6. W. Genthe and H. Hausner, Corrosion of Alumina in Acids, *Euro-ceramics 1*, Vol 3, Elvesier (London), 1989, p 463-467
7. J. Knuuttila, P. Sorsa, and T. Mäntylä, Sealing of Thermal Spray Coatings by Impregnation, *J. Thermal Spray Technol.*, 1999, **8**(2), p 249-257
8. R. Krishnan, S. Dash, R. Kesavamoorthy, C.B. Rao, A.K. Tyagi, and B. Raj, Laser Surface Modification and Characterization of Air Plasma Spray Coatings by Impregnation, *Surf. Coat. Technol.*, 2006, **200**(8), p 2791-2799
9. M. Vippola, S. Ahmaniemi, J. Keränen, P. Vuoristo, T. Lepistö, T. Mäntylä, and E. Olsson, Aluminum Phosphate Sealed Alumina Coating: Characterization of Microstructure, *Mater. Sci. Eng. A*, 2002, **323**(1-2), p 1-8
10. S. Liscano, L. Gil, and M. Staia, Effect of Sealing Treatment on the Corrosion Resistance of Thermal-Sprayed Ceramic Coating, *Surf. Coat. Technol.*, 2004, **188-189**, p 135-139
11. L.-M. Berger, Titanium Oxide—New Opportunities for an Established Coating Material, *Thermal Spray Solutions: Advances in Technology and Applications*, on CD-ROM, May 10-12, 2004 (Osaka, Japan), DVS-Verlag GmbH, Düsseldorf, 2004

12. R.S. Lima and B.R. Marple, Thermal Spray Coatings Engineered from Nanostructured Ceramic Agglomerated Powders for Structural, Thermal Barrier and Biomedical Applications: A Review, *J. Thermal Spray Technol.*, 2007, **16**(1), p 40-63
13. P.C.S. Hayfield, Development of a New Material—Monolithic Ti_4O_7 Ebonex® Ceramic, Cambridge, Herts: Royal Soc. Chem., Metal Finishing Information Services, 2002, 97 pp
14. J. Ilavsky, C.C. Berndt, H. Herman, P. Chraska, and J. Dubsky, Alumina-Base Plasma-Sprayed Materials—Part II: Phase Transformation in Aluminas, *J. Thermal Spray Technol.*, 1997, **6**(4), p 439-444
15. H. Kreye, Herstellung von Aluminiumoxidschichten mit verbesserten Eigenschaften (Preparation of Alumina Coatings with Improved Properties), University of the Federal Armed Forces Hamburg, Institute for Materials Technologies, Final Report, AiF founded Project No. 11.466 N, 01.01.1998-31.12.1999 (in German)
16. D. Yan, J. He, X. Li, Y. Liu, J. Zhang, and H. Ding, An Investigation of the Corrosion Behavior of Al_2O_3-Based Ceramic Composite Coatings in Dilute HCl Solution, *Surf. Coat. Technol.*, 2001, **141**, p 1-6
17. E. Çelik, I. Ozdemir, E. Avci, and Y. Tsunekawa, Corrosion Behaviour of Plasma Sprayed Coatings, *Surf. Coat. Technol.*, 2005, **193**, p 297-302
18. L. Beyerlein and E. Döpel, Aluminiumtitanatspritzpulver und seine Anwendung beim Plasmaspritzen (Aluminum Titanate Spray Powder and its Application in Plasma Spraying), *Schweißtechnik*, 1989, **39**(2), p 55-56 (in German)
19. J. Beczkowiak, H. Keller, and G. Schwier, Al_2O_3-TiO_2 Coatings—An Alternative to Cr_2O_3? *Thermische Spritzkonferenz 1996*, Düsseldorf, E. Lugscheider, Ed., DVS-Berichte 175, DVS-Verlag, 1996, p 68-75
20. L.-M. Berger, C.C. Stahr, F.-L. Toma, S. Saaro, M. Herrmann, D. Deska, and G. Michael, Korrosion thermisch gespritzter oxidkeramischer Schichten (Corrosion of Thermally Sprayed Oxide Ceramic Coatings), *Thermal Spray Bull.*, 2009, **2**(1), p 40-56
21. C.C Stahr, L.-M. Berger, F.-L. Toma, M. Herrmann, D. Deska, and G. Michael, Korrosion thermisch gespritzter Schichten auf der Basis von Aluminiumoxid (Corrosion of Thermally Sprayed Coatings Based on Aluminium Oxides), *Mat.-wiss. u. Werkstofftech.*, 2008, **39**(12), p 892-896 (in German)
22. L.-M. Berger, S. Saaro, C.C. Stahr, S. Thiele, and M. Woydt, Entwicklung keramischer Schichten im System Cr_2O_3-TiO_2 (Development of Ceramic Coatings in the Cr_2O_3-TiO_2 System), *Thermal Spray Bull.*, 2009, **2**(1), p 64-77
23. J. Schilm, M. Herrmann, and G. Michael, Corrosion of Si_3N_4-Ceramics in Aqueous Solutions Part 2. Corrosion Mechanisms in Acids as a Function of Concentration, Temperature and Composition, *J. Eur. Ceram. Soc.*, 2007, **27**(12), p 3573-3588
24. M. Harju, J. Halme, M. Järn, J.B. Rosenholm, and T. Mäntylä, Influence of Aqueous Aging on Surface Properties of Plasma Sprayed Oxide Coatings, *J. Colloid Interface Sci.*, 2007, **313**(1), p 194-201
25. E. Baumgarten, F.O. Geldsetzer, and U. Kirchhausen-Düsing, Investigation and Modelling of the γ-Al_2O_3/Water system, *J. Colloid Interface Sci.*, 1995, **173**(1), p 104-111